ASM Sc. J., 12, Special Issue 1, 2019 for IQRAC2018, 82-91

Numerical Solution for Circular Arc Cracks in Half Plane Elasticity

N. R. F. Elfakhakhre [2], N. M. A. Nik long [*1, 2], Z. K. Eshkuvatov [1, 3], and N. Senu[1, 2]

[1]*Institute for Mathematical Research, Universiti Putra Malaysia, 43400 UPM Serdang, Selangor, Malaysia*

[2]*Department of Mathematics, Faculty of Science, Universiti Putra Malaysia, 43400 UPM Serdang, Selangor, Malaysia*

[3]*Faculty of Science and Technology, Universiti Sains Islam Malaysia, 71800 Negeri Sembilan, Malaysia*

[*]*Corresponding author: nmasri@upm.edu.my*

Numerical solutions for an elastic half plane with circular arc cracks subjected to uniaxial tension $\sigma_x^{\infty} = p$ is presented. The free traction on the boundary of the half plane is assumed. Based on the modified complex potential and superposition method, the problem is formulated into a singular integral equation with the distribution dislocation function as unknown. Numerical examples exhibit the behavior of the stress intensity factor at the cracks tips for various positions. Our numerical results are in agreement with the existence one.

Keywords: stress intensity factor, singular integral equation, circular arc crack, half plane.

I. Introduction

The influences between cracks is one of the main factors in determining the component life of structures since the interaction of the cracks can significantly affect the stress intensity factors of the cracks. The stress intensity factor may increases or decreases. Due to this reason many researchers give a significant to develop the analytical methods to evaluate the stresses around multiple interacting cracks. Kachanov (2003) presented a short overview of several approaches for two and three dimensional crack interaction problems. Li et al. (2008) proposed a fast and accurate solution for crack interaction problems in infinite and half plane. Based on the method of complex potentials, the final solution is obtained via a perturbation approach.

A series of papers have been published to study the problem of three cracks as a special case of multiple cracks for several plane and different crack configurations. Three collinear, parallel, Griffith cracks problems are proposed for dissimilar piezoelectric materials, infinite and orthotropic elastic plane by Lam and Phua (1991), Itou and Haliding (1997), Das and Patra (1998), Das et al. (2001), Choi and Chung (2013), Itou (2016), Sadowski et al. (2016), and Akhtar and Hasan (2017). Chen and Hasebe (1997) and Yan (2010) proposed three circular arc cracks problem in an infinite plate by using Fredholm integral equation and boundary element method, respectively. Moreover, Bagheri (2017) determined the dynamic field stress intensity factors for three horizontal cracks by using the numerical Laplace inversion and dislocation densities. In addition Elfakhakhre et al. (2018) solved the interaction of two curved cracks problem in half plane elasticity.

In this paper, a numerical approach for analyzing interacting three circular arc cracks in an elastic half plane is considered. The behavior of the stress intensity factor at the crack tips subjected to uniaxial tension $\sigma_x^{\infty} = p$ with free traction boundary condition in half plane elasticity. The problem is formulated into singular integral equations with the distribution

dislocation function as unknown. In the formulation, we make use the modified complex potential. The appropriate quadrature formulas together with a suitable choice of collocation points, the singular integral equations are reduced to the system of linear equations for the unknown coefficients. Numerical examples exhibit the values of stress intensity factor are influenced by the distance between the cracks.

II. The problem formulation

Assume that three circular arc cracks lie on the upper half plane with the same radius R subjected to uniaxial tension $\sigma_x^{\infty} = p$ as shown in Figure 1. To solve this problem, Muskhelishvili's method for plane elasticity is utilized (Muskhelishvili (1953)). Based on this method, the stresses $(\sigma_x, \sigma_y, \sigma_{xy})$, the resultant forces (X, Y) and the displacements (u, v) can be described used two complex potentials $\Phi(z) = \phi^{'}(z)$ and $\Psi(z) = \psi^{'}(z)$ as

$$\sigma_x + \sigma_y = 4Re[\Phi(z)], \tag{1}$$

$$\sigma_y - i\sigma_{xy} = 2Re\Phi(z) + z\overline{\Phi^{'}(z)} + \overline{\Psi(z)}, \tag{2}$$

$$f = -Y + iX = \phi(z) + z\overline{\phi^{'}(z)} + \overline{\psi(z)}, \tag{3}$$

$$2G(u + iv) = \kappa\phi(z) - z\overline{\phi^{'}(z)} - \overline{\psi(z)}, \tag{4}$$

where G is shear modulus of elasticity, $\kappa = (3 - v)/(1 + v)$ in the plane stress problem, $\kappa = 3 - 4v$ in the plane strain problem, v is the Poisson's ratio, and a bar over a function denotes the conjugated value for the function. The derivative in a specified direction (abbreviated as DISD) is defined as

$$\begin{aligned} N + iT &= \frac{d}{dz}(-Y + iX) \\ &= \Phi(z) + \overline{\Phi(z)} + \frac{d\bar{z}}{dz}\left(z\overline{\Phi^{'}(z)} + \overline{\Psi(z)}\right), \end{aligned} \tag{5}$$

where $N + iT$ denotes the normal and tangential tractions along the crack segment $\overline{z, z + dz}$. The value of $N + iT$ depends on the positions of point z as well as on the direction of the segment $d\bar{z}/dz$.

The problem is formulated as a special case for multiple curved cracks problem (Elfakhakhre et al. (2018)). By consider the distribution dislocation functions $g_1'(t_1)$, $g_2'(t_2)$, and $g_3'(t_3)$, respectively, for crack-1 (L_1), crack-2 (L_2), and crack-3 (L_3). Let $N_k(t_{k0}) + iT_k(t_{k0})$ be the tractions applied on the crack-k at the point t_{k0} for $k = 1, 2, 3$, then the equations for the three cracks subjected to traction can be written as follow

$$\begin{aligned} &\frac{1}{\pi}\int_{L_k}\frac{g_k'(t_k)dt_k}{t_k - t_{k0}} + \frac{1}{2\pi}\left(\int_{L_k} B_1(t_k, t_{k0})g_k'(t_k)dt_k + \right. \\ &\left.\int_{L_k} B_2(t_k, t_{k0})\overline{g_k'(t_k)}d\bar{t_k}\right) + \sum_{j=1}^{3}{}'\left[\frac{1}{\pi}\int_{L_j}\frac{g_j'(t_j)dt_j}{t_j - t_{k0}}\right. \\ &+ \frac{1}{2\pi}\left(\int_{L_j} B_1(t_j, t_{k0})g_j'(t_j)dt_j + \right. \\ &\left.\left.\int_{L_j} B_2(t_j, t_{k0})\overline{g_j'(t_j)}d\bar{t_j}\right)\right] = N_k(t_{k0}) + iT_k(t_{k0}), \end{aligned} \tag{6}$$

where the function $g'(t_k)$ is defined as

$$\begin{aligned} g'(t_k) = -\frac{2Gi}{\kappa + 1}\frac{d}{dt_k}\Big\{&(u(t_k) + iv(t_k))^{+} \\ &- (u(t_k) + iv(t_k))^{-}\Big\}, \end{aligned} \tag{7}$$

where $t_k \in L_k$, the subscript (+) (or (-)) mean the upper (or lower) face of each crack, and $((u(t_k)+iv(t_k))^{+} - (u(t_k)+iv(t_k))^{-})$ represents the displacements at a point t_k of the upper and lower faces of each crack L_k. In Equation (7) the expression $d\{\}/dt$ should be defined as in Muskhelishvili (1953) and Chen et al. (2003). In Equation (6) the kernels are expressed as follow

$$\begin{aligned} B_1(t_j, t_{k0}) &= A_1(t_j, t_{k0}) + A_3(t_j, t_{k0}) + A_5(t_j, t_{k0}), \\ B_2(t_j, t_{k0}) &= A_2(t_j, t_{k0}) + A_4(t_j, t_{k0}) + A_6(t_j, t_{k0}), \\ &\text{for } k, j = 1, 2, 3, \end{aligned}$$

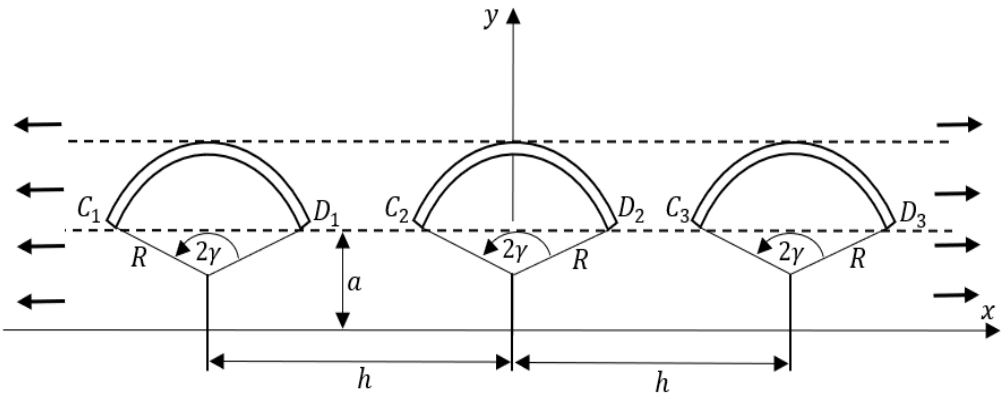

Figure 1: Three collinear circular arc cracks in an elastic half plane.

and

$$A_1(t_j,t_{k0}) = -\frac{1}{t_j - t_{k0}} + \frac{1}{\overline{t_j} - \overline{t_{k0}}}\frac{d\overline{t_{k0}}}{dt_{k0}},$$

$$A_2(t_j,t_{k0}) = \frac{1}{\overline{t_j} - \overline{t_{k0}}} - \frac{t_j - t_{k0}}{(\overline{t_j} - \overline{t_{k0}})^2}\frac{d\overline{t_{k0}}}{dt_{k0}},$$

$$A_3(t_j,t_{k0}) = -\frac{1}{\overline{t_j} - t_{k0}} + \frac{\overline{t_j} - t_j}{(t_j - \overline{t_{k0}})^2},$$

$$A_4(t_j,t_{k0}) = -\frac{1}{t_j - \overline{t_{k0}}} + \frac{t_j - \overline{t_j}}{(\overline{t_j} - t_{k0})^2},$$

$$A_5(t_j,t_{k0}) = \frac{d\overline{t_{k0}}}{dt_{k0}}\left(\frac{2t_{k0}(\overline{t_j} - t_j)}{(t_j - \overline{t_{k0}})^3} + \frac{(3\overline{t_{k0}} - \overline{t_j})}{(t_j - \overline{t_{k0}})^2} + \frac{2\overline{t_{k0}}(\overline{t_{k0}} - \overline{t_j})}{(t_j - \overline{t_{k0}})^3}\right),$$

$$A_6(t_j,t_{k0}) = \frac{d\overline{t_{k0}}}{dt_{k0}}\left(\frac{t_j - t_{k0}}{(t_j - \overline{t_{k0}})^2}\right).$$

Note that in Equation (6) the symbol $\sum'$ denotes the terms corresponding to $j = k$ are excluded, and the first three integrals represent to the effect on crack-k caused by the dislocations on the crack-k itself, whereas the other three integrals denote the effect of the dislocations on crack-j where $j = 1, 2, 3, j \neq k$. In addition, the single-valuedness conditions of displacement dislocation functions $g'_k(t_k)$ are defined as

$$\int_{L_k} g'_k(t_k)dt_k = 0, \text{ for } k = 1, 2, 3. \qquad (8)$$

In solving Equation (6) subjected to Equation (8), we map the cracks on a real axis by s_k with intervals of $2b_k$ for crack-k, $k = 1, 2, 3$. The mappings are expressed as (Chen (2004))

$$g'_k(t_k)|_{t_k = t_k(s_k)} = h_k(s_k) = \frac{H_k(s_k)}{\sqrt{b_k^2 - s_k^2}}, \qquad (9)$$
$$\text{where} \quad H_k(s_k) = H_{k1}(s_k) + iH_{k2}(s_k).$$

The following Gauss integration rules (Erdogan et al. (1973)) are also used in solving the integral equations

$$\frac{1}{\pi}\int_{-b}^{b} \frac{F(s)}{\sqrt{b^2 - s^2}(s - s_{0,m})}ds = \frac{1}{M}\sum_{i=1}^{M}\frac{F(s_i)}{(s_i - s_{0,m})}, \qquad (10)$$

$$\frac{1}{\pi}\int_{-b}^{b} \frac{F(s)}{\sqrt{b^2 - s^2}}ds = \frac{1}{M}\sum_{i=1}^{M} F(s_i), \qquad (11)$$

where M is some integer, and

$$s_i = b\cos\frac{(i - 0.5)\pi}{M},$$
$$s_{0,m} = b\cos\frac{m\pi}{M},$$
$$\text{for } i = 1, 2, \ldots, M, \text{ and } m = 1, 2, \ldots, M - 1. \qquad (12)$$

III. NUMERICAL EXAMPLES

The stress intensity factor (SIF) at the crack tips C_1 and D_1 of crack-1, C_2 and D_2 of crack-2, and C_3 and D_3 of crack-3 (Figure 1) can be evaluated as follow (Chen (2004))

$$(K_1 - iK_2)_{C_k} = \sqrt{2\pi} \lim_{t \to t_{C_k}} \sqrt{|t - t_{C_k}|} g_k'(t) = \sqrt{\frac{\pi}{b_k}} H_k(-b_k), \quad k = 1, 2, 3, \tag{13}$$

$$(K_1 - iK_2)_{D_k} = -\sqrt{2\pi} \lim_{t \to t_{D_k}} \sqrt{|t - t_{D_k}|} g_k'(t) = -\sqrt{\frac{\pi}{b_k}} H_k(b_k), \quad k = 1, 2, 3. \tag{14}$$

A. Example 1

Assume that three collinear circular arc cracks of angle 2γ lie in upper half plane as seen in Figure 1 with radius R and free traction on the boundary. The cracks subjected to the remote tension $\sigma_x^\infty = p$. The SIFs at the cracks tips are expressed as

$$\begin{aligned} K_{1C_k} &= F_{1C_k}(a/R, 2b/h)\sigma_x^\infty \sqrt{\pi b}, \\ K_{2C_k} &= F_{2C_k}(a/R, 2b/h)\sigma_x^\infty \sqrt{\pi b}, \\ K_{1D_k} &= F_{1D_k}(a/R, 2b/h)\sigma_x^\infty \sqrt{\pi b}, \\ K_{2D_k} &= F_{2D_k}(a/R, 2b/h)\sigma_x^\infty \sqrt{\pi b}, \\ \text{where } b &= R\sin(\gamma) \text{ for } k = 1, 2, 3. \end{aligned} \tag{15}$$

The calculated SIFs at the cracks tips C_1, D_1, and C_2 are listed in Table 1, which illustrates the variation of the SIFs with $a/R = 0.2, 0.4, \ldots, 2.0$ and the dimensionless distance $2b/h = 0.1, 0.5, 0.9$ for $\gamma = 90°$, where a is the distance between the cracks tips and the boundary of half plane. Note that, $F_{1C_1} = F_{1D_3}$, $F_{1D_1} = F_{1C_3}$, $F_{1C_2} = F_{1D_2}$, $F_{2C_1} = -F_{2D_3}$, $F_{2D_1} = -F_{2C_3}$, and $F_{2C_2} = -F_{2D_2}$. In the case $2b/h = 0.1$, the data in Table 1 are compared with those of Elfakhakhre et al. (2018) for a half circular arc crack, it is found to be in good agreement. It indicates that in the case $2b/h = 0.1$ the interaction between three circular arc cracks is negligible, and our numerical results are reliable. Observed that the SIFs at crack tips C_1 and C_2 decrease as the $2b/h$ increases but at D_1 there is slightly disturbance. Whereas the SIFs increase as a/R decreases. Figure 2 shows that the SIFs increases as the half opening crack angle (γ) increases for $a/R = 0.2$ and $2b/h = 0.9$.

B. Example 2

Assume that three collinear circular arc cracks of angle 2γ lie in upper half plane as seen in Figure 3 with the same radius R and free traction on the boundary. The cracks subjected to the remote tension $\sigma_x^\infty = p$. The SIFs at the

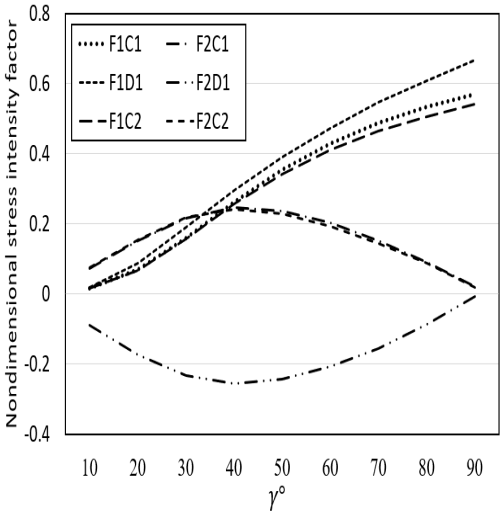

Figure 2: Nondimensional SIFs for three circular arc crack in an elastic half plane when $a/R = 0.2$ and $2b/h = 0.9$ (Figure 1).

Table 1: Nondimensional SIFs for three circular arc cracks in an elastic half plane (Figure 1).

		a/R									
	$2b/h$	0.2	0.4	0.6	0.8	1.0	1.2	1.4	1.6	1.8	2.0
F_{1C_1}											
	0.1	0.7563	0.7164	0.6945	0.6797	0.6703	0.6644	0.6605	0.6581	0.6564	0.6551
	0.5	0.6908	0.6676	0.6494	0.6338	0.6225	0.6150	0.6096	0.6059	0.6031	0.6007
	0.9	0.5706	0.5370	0.5090	0.4868	0.4713	0.4611	0.4544	0.4501	0.4473	0.4452
F_{1D_1}											
	0.1	0.7559	0.7159	0.6938	0.6788	0.6692	0.6632	0.6592	0.6566	0.6549	0.6534
	0.5	0.6716	0.6529	0.6472	0.6439	0.6421	0.6412	0.6405	0.6401	0.6398	0.6393
	0.9	0.6665	0.6685	0.6710	0.6705	0.6687	0.6665	0.6637	0.6609	0.6583	0.6556
F_{1C_2}											
	0.1	0.7531	0.7135	0.6917	0.6770	0.6675	0.6617	0.6579	0.6554	0.6538	0.6525
	0.5	0.6415	0.6343	0.6270	0.6184	0.6112	0.6058	0.6015	0.5983	0.5958	0.5935
	0.9	0.5426	0.5246	0.5049	0.4871	0.4739	0.4649	0.4587	0.4547	0.4519	0.4499
F_{2C_1}											
	0.1	0.0100	0.0215	0.0334	0.0439	0.0517	0.0570	0.0602	0.0621	0.0631	0.0635
	0.5	0.0070	0.0167	0.0262	0.0346	0.0413	0.0462	0.0497	0.0521	0.0537	0.0547
	0.9	0.0208	0.0581	0.0772	0.0886	0.0962	0.1017	0.1058	0.1090	0.1115	0.1136
F_{2D_1}											
	0.1	-0.0101	-0.0216	-0.0336	-0.0441	-0.0520	-0.0574	-0.0607	-0.0626	-0.0636	-0.0641
	0.5	-0.0088	-0.0201	-0.0308	-0.0394	-0.0453	-0.0489	-0.0508	-0.0517	-0.0520	-0.0520
	0.9	-0.0054	-0.0146	-0.0238	-0.0312	-0.0361	-0.0389	-0.0404	-0.0412	-0.0416	-0.0419
F_{2C_2}											
	0.1	0.0088	0.0204	0.0323	0.0428	0.0507	0.0560	0.0593	0.0612	0.0622	0.0627
	0.5	0.0075	0.0171	0.0254	0.0318	0.0364	0.0395	0.0417	0.0433	0.0445	0.0454
	0.9	0.0201	0.0557	0.0702	0.0774	0.0823	0.0864	0.0902	0.0939	0.0972	0.1003
F^*_{1C}		0.7611	0.7205	0.6981	0.6831	0.6733	0.6672	0.6632	0.6605	0.6586	0.6572
F^*_{2C}		0.0089	0.0206	0.0326	0.0432	0.0511	0.0564	0.0597	0.0616	0.0626	0.0631

* The SIFs value for a half circular arc crack (Elfakhakhre et al. (2018))

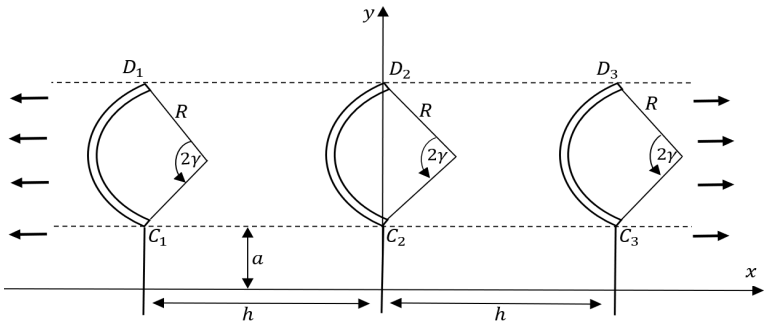

Figure 3: Three circular arc cracks in upper elastic half plane.

Table 2: Nondimensional SIFs at the crack tips C_1 and D_1 for three circular arc cracks in an elastic half plane (Figure 3).

		$\gamma(^\circ)$					
	$2b/h$	15	30	45	60	75	90
F_{1C_1}							
	0.1	1.3586	1.0720	0.6662	0.2213	-0.1569	-0.1901
	0.5	1.3275	0.9994	0.6057	0.2078	-0.1557	-0.1901
	0.9	1.2750	0.9310	0.5515	0.1622	-0.1267	-0.1901
F_{1D_1}							
	0.1	1.0946	0.9078	0.6449	0.3524	0.0545	-0.0255
	0.5	1.0676	0.8305	0.5325	0.2328	0.0163	-0.0255
	0.9	1.0262	0.7703	0.4730	0.2068	-0.0533	-0.0255
F_{2C_1}							
	0.1	0.4008	0.7472	0.9373	0.9553	0.7744	0.2045
	0.5	0.4032	0.6725	0.7867	0.7664	0.5999	0.2045
	0.9	0.3769	0.6010	0.7258	0.7272	0.6096	0.2045
F_{2D_1}							
	0.1	-0.2675	-0.5092	-0.6544	-0.6999	-0.6334	-0.2023
	0.5	-0.2787	-0.4992	-0.6222	-0.6106	-0.4583	-0.2023
	0.9	-0.2847	-0.4994	-0.5890	-0.5591	-0.4076	-0.2023

cracks tips are expressed as

$$\begin{aligned} K_{1C_k} &= F_{1C_k}(\gamma, 2b/h)\sigma_x^\infty\sqrt{\pi b}, \\ K_{2C_k} &= F_{2C_k}(\gamma, 2b/h)\sigma_x^\infty\sqrt{\pi b}, \\ K_{1D_k} &= F_{1D_k}(\gamma, 2b/h)\sigma_x^\infty\sqrt{\pi b}, \\ K_{2D_k} &= F_{2D_k}(\gamma, 2b/h)\sigma_x^\infty\sqrt{\pi b}, \\ \text{where } b &= R\sin(\gamma) \text{ for } k = 1, 2, 3. \end{aligned} \tag{16}$$

The calculated SIFs at the cracks tips are given in Table 2, Table 3, and Table 4 in which illustrate the variation of the SIFs with $\gamma = 15^\circ, 30^\circ, 45^\circ, 60^\circ, 75^\circ, 90^\circ$ and dimensionless distance $2b/h = 0.1, 0.5, 0.9$ for $a = 0.2R\sin(\gamma)$, where a is defined as in Figure 3. In the case $2b/h = 0.1$ and $\gamma = 15^\circ$, the data in Tables 2, 3, and 4 are compared with those of Chen et al. (2009) for an arc crack, and it is found that the agreement is very good. Note that, in the case of an arc crack in an infinite plate we have

$$\begin{aligned} F1C(a/R)_{a/R=0.2} &= 1.3609, \\ F2C(a/R)_{a/R=0.2} &= 0.4154, \\ F1D(a/R)_{a/R=0.2} &= 1.0953 \\ F2D(a/R)_{a/R=0.2} &= -0.2792. \end{aligned}$$

It indicates that in the case $2b/h = 0.1$ the interaction between three circular arc cracks is negligible, and our numerical results are reliable. Note that the effect of interaction is nonexistent between the cracks when $\gamma = 90^\circ$.

C. Example 3

Consider three circular arc cracks of angle 2γ lie in upper half plane (Figure 4) with the radius R_1, R_2, and R_3, and $R_1/R_2 = R_2/R_3 = \lambda$. The cracks subjected to the remote tension $\sigma_x^\infty = p$ and free boundary condition. The SIFs at the cracks tips are expressed as

Table 3: Nondimensional SIFs at the crack tips C_2 and D_2 for three circular arc cracks in an elastic half plane (Figure 3).

		$\gamma(^\circ)$					
	$2b/h$	15	30	45	60	75	90
F_{1C_2}							
	0.1	1.3582	1.0684	0.6592	0.2084	-0.1843	-0.1901
	0.5	1.3058	0.9348	0.5240	0.1939	0.0409	-0.1901
	0.9	1.2750	0.9310	0.5515	0.1622	-0.1267	-0.1901
F_{1D_2}							
	0.1	1.0937	0.9055	0.6419	0.3553	0.0964	-0.0255
	0.5	1.0546	0.8206	0.5633	0.3125	0.1288	-0.0255
	0.9	1.0021	0.7786	0.5224	0.2921	0.0617	-0.0255
F_{2C_2}							
	0.1	0.4146	0.7445	0.9301	0.9353	0.7220	0.2045
	0.5	0.3987	0.6545	0.7506	0.7289	0.5884	0.2045
	0.9	0.3726	0.5854	0.6880	0.6790	0.5063	0.2045
F_{2D_2}							
	0.1	-0.2787	-0.5067	-0.6482	-0.6855	-0.6157	-0.2023
	0.5	-0.2690	-0.4638	-0.5722	-0.5456	-0.3889	-0.2023
	0.9	-0.2569	-0.4375	-0.4967	-0.4484	-0.3414	-0.2023

Table 4: Nondimensional SIFs at the crack tips C_3 and D_3 for three circular arc cracks in an elastic half plane (Figure 3).

		$\gamma(^\circ)$					
	$2b/h$	15	30	45	60	75	90
F_{1C_3}							
	0.1	1.3587	1.0716	0.6633	0.2065	-0.2293	-0.1901
	0.5	1.3250	0.9717	0.5303	0.1634	0.0351	-0.1901
	0.9	1.2647	0.8751	0.5250	0.3066	0.1002	-0.1901
F_{1D_3}							
	0.1	1.0946	0.9085	0.6495	0.3742	0.1530	-0.0255
	0.5	1.0717	0.8706	0.6385	0.4155	0.2422	-0.0255
	0.9	1.0419	0.8524	0.6407	0.4415	0.2591	-0.0255
F_{2C_3}							
	0.1	0.4057	0.7477	0.9391	0.9593	0.7725	0.2045
	0.5	0.4078	0.7044	0.8310	0.7945	0.7116	0.2045
	0.9	0.4011	0.6647	0.7573	0.7575	0.7110	0.2045
F_{2D_3}							
	0.1	-0.2713	-0.5085	-0.6523	-0.6972	-0.6450	-0.2023
	0.5	-0.2676	-0.4579	-0.5697	-0.6000	-0.5712	-0.2023
	0.9	-0.2453	-0.4143	-0.5155	-0.5530	-0.5627	-0.2023

Table 5: Nondimensional SIFs for three circular arc cracks with different radius in an elastic half plane (Figure 4).

		λ								
	$\gamma(^\circ)$	0.1	0.2	0.3	0.4	0.5	0.6	0.7	0 .8	0.9
F_{1C_1}	30	0.0262	0.0212	0.0204	0.0244	0.0339	0.0506	0.0758	0.1036	0.1394
	60	0.2276	0.2313	0.2453	0.2634	0.2798	0.2909	0.2990	0.3095	0.3126
	90	0.5545	0.5533	0.5585	0.5654	0.5648	0.5520	0.5319	0.5195	0.5154
F_{1C_2}										
	30	0.0697	0.0653	0.0619	0.0592	0.0578	0.0610	0.0734	0.0944	-0.0751
	60	0.3564	0.3503	0.3465	0.3385	0.3265	0.3132	0.3020	0.2926	0.2587
	90	0.6623	0.6422	0.6195	0.5884	0.5508	0.5137	0.4857	0.4643	0.4136
F_{1C_3}										
	30	0.1940	0.1930	0.1906	0.1858	0.1769	0.1621	0.1431	0.1299	0.1841
	60	0.5138	0.5103	0.5041	0.4944	0.4799	0.4576	0.4234	0.3789	0.3622
	90	0.7572	0.7468	0.7308	0.7098	0.6838	0.6510	0.6074	0.5503	0.5026
F_{2C_1}										
	30	0.1302	0.1366	0.1465	0.1582	0.1717	0.1849	0.1904	0.1780	0.1461
	60	0.2285	0.2175	0.2014	0.1865	0.1743	0.1668	0.1668	0.1747	0.1764
	90	0.1134	0.1002	0.0742	0.0492	0.0286	0.0173	0.0167	0.0294	0.0596
F_{2C_2}										
	30	0.1552	0.1618	0.1725	0.1854	0.1979	0.2052	0.1982	0.1703	0.1518
	60	0.2104	0.1951	0.1827	0.1736	0.1682	0.1677	0.1713	0.1662	0.1374
	90	0.0526	0.0411	0.0280	0.0190	0.0136	0.0124	0.0164	0.0219	0.0127
F_{2C_3}										
	30	0.2360	0.2352	0.2334	0.2301	0.2240	0.2138	0.1993	0.1842	0.2120
	60	0.2262	0.2245	0.2219	0.2184	0.2137	0.2071	0.1969	0.1787	0.1520
	90	0.0089	0.0090	0.0095	0.0105	0.0124	0.0150	0.0168	0.0097	-0.0276

$$
\begin{aligned}
K_{1C_k} &= F_{1C_k}(\gamma,\lambda)\sigma_x^\infty\sqrt{\pi b},\\
K_{2C_k} &= F_{2C_k}(\gamma,\lambda)\sigma_x^\infty\sqrt{\pi b},\\
K_{1D_k} &= F_{1D_k}(\gamma,\lambda)\sigma_x^\infty\sqrt{\pi b},\\
K_{2D_k} &= F_{2D_k}(\gamma,\lambda)\sigma_x^\infty\sqrt{\pi b},\\
\text{where } b &= R\sin(\gamma) \text{ for } k=1,2,3.
\end{aligned}
\tag{17}
$$

The calculated SIFs at the cracks tips are given in Table 5, which illustrates the variation of the SIFs with $\gamma = 30^\circ, 60^\circ, 90^\circ$ and $\lambda = 0.1, 0.2, \ldots, 0.9$ for $a = 0.2$, where a is defined as in Figure 4. Observed that at the crack tip C_3 for $\lambda = 0.1$ and $\gamma = 90^\circ$ the data in Table 5 are compared with those of Elfakhakhre et al. (2018) for a half circular arc crack (see Table 1), and it is found to be in good agreement. It indicates that in the case $\lambda = 0.1$ the interaction between three circular arc cracks is negligible, and our numerical results are reliable. Note that the SIFs increase as γ increases.

IV. CONCLUSION

Several situations in fracture mechanics involve a complicated arrangement of cracks that is not easy to analysis due to the interaction between the cracks with each other. However, the singular integral equations were formulated for three circular arc cracks in an elastic half plane. For

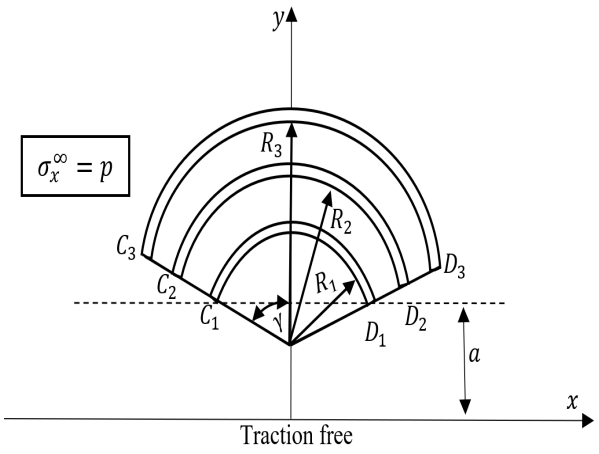

Figure 4: Three circular arc cracks in upper elastic half plane with different radius.

numerical purpose we apply the curve coordinate method and appropriate quadrature rules. The several numerical results exhibit the effectiveness of this approach and also illustrate the effect of the cracked geometry on the stress intensity factor. We can conclude that the stress intensity factor is influenced by the distance between cracks, distance between cracks and boundary, and the position and configurations of the cracks.

ACKNOWLEDGEMENTS

The author would like to thank University Putra Malaysia for the Putra Grant, Vot No. 9567900.

References

[1] N. Akhtar and S. Hasan. Assessment of the interaction between three collinear unequal straight cracks with unified yield zones. *AIMS Materials Science*, 4:302–316, 2017.

[2] R. Bagheri. Several horizontal cracks in a piezoelectric half-plane under transient loading. *Archive of Applied Mechanics*, 87:1979–1992, 2017.

[3] Y. Z. Chen. Solution of integral equation in curve crack problem by using curve length coordinate. *Engineering Analysis Boundary Elements*, 28:989–994, 2004.

[4] Y. Z. Chen and N. Hasebe. Fredholm integral equation for the multiple circular arc crack problem in plane elasticity. *Archive of Applied Mechanics*, 67: 433–446, 1997.

[5] Y. Z. Chen, N. Hasebe, and K. Y. Lee. *Multiple Crack Problems in Elasticity.* WIT Press, Southampton, 2003.

[6] Y. Z. Chen, X. Y. Lin, and X. Z. Wang. Numerical solution for curved crack problem in elastic half-plane using hypersingular integral equation. *Philosophical Magazine*, 89(26):2239–2253, 2009.

[7] S. R. Choi and I. Chung. Analysis of three collinear antiplane interfacial cracks in dissimilar piezoelectric materials under non-self equilibrated electromechanical loadings on a center crack. *Journal of Mechanical Science and Technology*, 27:3097–3101, 2013.

[8] S. Das and B. Patra. Interaction between three line cracks in a sandwiched orthotropic layer. *Applied Mechanics and Engineering*, 3(2):249–269, 1998.

[9] S. Das, B. Patra, and L. Debnath. Interaction between three moving Griffith cracks at the interface of two dissimilar elastic media. *Korean Journal of Computational and Applied Mathematics*, 8(1): 59–69, 2001.

[10] N. R. F. Elfakhakhre, N. M. A. Nik Long, and Z. K. Eshkuvatov. Stress intensity factor for an elastic half plane weakened by multiple curved cracks. *Applied Mathematical Modelling*, 60:540–551, 2018.

[11] F. Erdogan, G. D. Gupt, and T. S. Cook. Numerical solution of singular integral

equation. In G. C. Sih, editor, *Mechanics of Fracture*, pages 368–425. Leyden Noordhoff, 1973.

[12] S. Itou. Dynamic stress intensity factors of three collinear cracks in an orthotropic plate subjected to time-harmonic disturbance. *Journal of Mechanics*, 32:491–499, 2016.

[13] S. Itou and H. Haliding. Dynamic stress intensity factors around three cracks in an infinite elastic plane subjected to time-harmonic stress waves . *International Journal of Fracture*, 83:379–391, 1997.

[14] M. Kachanov. On the problems of crack interactions and crack coalescence. *International Journal of Fracture*, 120:537–543, 2003.

[15] K. Y. Lam and S. P. Phua. Multiple crack interaction and its effect on stress intensity factor. *Engineering Fracture Mechanics*, 40:585–592, 1991.

[16] D. F. Li, C. F. Li, S. Q. Shu, Z. X. Wang, and J. Lu. A fast and accurate analysis of the interacting cracks in linear elastic solids. *International Journal of Fracture*, 151:169–185, 2008.

[17] N. I. Muskhelishvili. *Some Basic Problems of Mathematical Theory of Elasticity.* Noordhoff International Publishing, Leyden, The Netherlands, 1953.

[18] T. Sadowski, E. M. Craciun, A. Rabaea, and L. Marsavina. Mathematical modeling of three equal collinear cracks in an orthotropic solid. *Meccanica*, 51:329–339, 2016.

[19] X. Yan. A boundary element analysis for stress intensity factors of multiple circular arc cracks in a plane elasticity plate . *Applied Mathematical Modelling*, 34: 2722–2737, 2010.